COMPUTATIONAL MECHANICS
WCCM VI in conjunction with APCOM'04, *Sept. 5-10, 2004, Beijing, China*

Inverse Determination of Steady Boundary Conditions in Heat Transfer and Elasticity

George S. Dulikravich[1*], Brian H. Dennis[2], Thomas J. Martin[3]
[1] *Department of Mechanical and Materials Engineering, MAIDROC, Florida International University, 10555 W. Flagler St., Miami, Florida 33174, U.S.A.*
[2] I*nstitute of Environmental Studies, Graduate School of Frontier Science, University of Tokyo, 7-3-1 Hongo, Bunkyo-ku, Tokyo 113-8656, JAPAN*
[3] *Turbine Discipline Eng. & Systems Optimization Group, Pratt & Whitney Aircraft Co., 400 Main St., M/S 165-16, East Hartford, CT 06108, U. S. A.*
e-mail: dulikrav@fiu.edu, dennis@garlic.q.t.u-tokyo.ac.jp, thomas.martin@pw.utc.com

Abstract In the case of steady heat conduction and steady elasticity there is often a problem of not knowing temperatures and heat fluxes or tractions and deformations boundary conditions on some parts of the boundary. However, there should be a sufficient amount of over-specified boundary conditions available on at least a portion of the remaining boundary. . In this case, the entire process of determining the boundary conditions is of a truly non-destructive nature since there is no need to have values of the field variables at points inside the object. These problems can be solved either non-iteratively using a boundary element formulation or iteratively using a finite element formulation. In the case of a non-iterative formulation the solution process is very simple and numerical results are practically guaranteed. In the case of an iterative formulation, a judicious application of appropriate regularization algorithms must be performed. Furthermore, the over-specified boundary conditions must be highly accurate. Both algorithms have been demonstrated to work on simply-connected and multiply-connected two-and-three-dimensional configurations.

Key words: inverse problems, heat transfer, elasticity, regularization, SVD algorithm

INTRODUCTION

In this paper, we present a concise summary of analytical formulations, numerical implementations, results and experiences from our own research [1-10] in the general area of inverse determination of boundary conditions of multiply-connected arbitrarily shaped domains having fixed geometries. This class of problems arises very often in engineering practice when boundary values of certain field quantities cannot be measured on some parts of the boundary of an object. These situations often occur because of the inaccessibility of such boundaries to experimental apparatuses, because of the volatile and harsh environment that exists on these boundaries that could cause the measuring sensors to malfunction or even become damaged, etc. The methodologies to be discussed briefly are applicable to determining boundary values of any field variable, although we will offer examples of their applications in heat transfer and linear elasticity only.

BOUNDARY ELEMENT FORMULATION

The Boundary Element Method (BEM) [11], when used for linear boundary value problems, is a non-iterative solution procedure. If the global domain does not have too many subdomains, the BEM is significantly faster and more robust than the other numerical solution techniques. Analytical solutions to the partial differential equations governing the field variables, in the form of the Green's function, are a part of

the BEM solution. Introducing the Green's functions does not introduce any error into the solution thus guaranteeing high accuracy of the BEM. Furthermore, the non-iterative nature of the BEM eliminates stability, numerical dissipation and convergence problems and also removes any need for artificial dissipation. This is valuable because iterative inverse problem solving procedures like Finite Element Methods (FEM) [12] tend to amplify errors thus requiring complex regularization (smoothing) algorithms [13].

We will sketch the BEM in case of heat conduction equation for the steady-state temperature distribution, T(**x**), in a solid isotropic domain Ω bounded by the boundary Γ is given by

$$\nabla \cdot \left(k(T) \nabla T(\boldsymbol{x}) \right) + S(\boldsymbol{x}) = 0 \tag{1}$$

Here, *k(T)* is the temperature-dependent coefficient of thermal conductivity, **x** is the position vector, and *S(**x**)* is a function representing arbitrarily distributed heat sources (or sinks) per unit volume. Eq. (1) can be subject to the Dirichlet (temperature, *T*) boundary conditions on some parts of the boundary, the Neumann (heat flux, Q) boundary conditions on the other parts of the boundary, radiation heat flux conditions on yet another part of the boundary, and, when a boundary is exposed to a moving fluid, the Robin (convective heat transfer) boundary conditions on the remaining boundary, Γ_{conv},

$$-k \left. \frac{\partial T}{\partial n} \right|_{\Gamma_{conv}} = h_{conv} \left(T \big|_{\Gamma_{conv}} - T_{amb} \right) \tag{2}$$

Here, n is the direction of the outward normal to the boundary, h_{conv} is the local convective heat transfer coefficient, and T_{amb} is the ambient fluid temperature. Kirchhoff defined the non-dimensional temperature, u(**x**), as

$$u(x) = \int_{o}^{T} \frac{k(T)}{k_o} \frac{dT}{(T_{max} - T_{min})} \tag{3}$$

where k_O = constant is the reference value of the coefficient of thermal conductivity. The Eq. (1) then becomes Poisson's equation for the non-dimensional temperature *u(**x**)*.

$$\nabla^2 u(\boldsymbol{x}) + b(\boldsymbol{x}) = 0 \tag{4}$$

Here, the non-dimensionalized distributed heat source function is defined as

$$b(\boldsymbol{x}) = \frac{S(\boldsymbol{x})}{k_o} \frac{\ell^2}{(T_{max} - T_{min})} \tag{5}$$

where ℓ is the characteristic length. The Neumann boundary conditions can be transformed in terms of Kirchhoff's non-dimensional flux, *q*, as

$$q = \frac{\partial u}{\partial n} \tag{6}$$

The weighted residual statement minimizes this error by setting the weighted sum of the residuals over the entire domain and in the boundary conditions to zero. For Poisson's equation, the weighted residual statement is

$$\int_{\Omega} \left(\nabla^2 u(\mathbf{y}) + b(\mathbf{y})\right) w(\mathbf{x},\mathbf{y})\, d\Omega(\mathbf{y}) + \int_{\Gamma_1} \left(u(\mathbf{y}) - \bar{u}(\mathbf{y})\right) \frac{\partial w(\mathbf{x},\mathbf{y})}{\partial n}\, d\Gamma(\mathbf{y}) - \int_{\Gamma_2} \left(q(\mathbf{y}) - \bar{q}(\mathbf{y})\right) w(\mathbf{x},\mathbf{y})\, d\Gamma(\mathbf{y}) = 0 \tag{7}$$

Here, w(**x,y**) is the weighting function, **x** is the real space coordinate and **y** is the coordinate of local integration. Performing integration by parts twice on this equation amounts to Green's second identity [19, 20], retaining the Cauchy principal value of the boundary integrals, and using the properties of the Dirac delta function, the following Boundary Integral Equation (BIE) is obtained [18]

$$c(\mathbf{x})u(\mathbf{x}) + \int_{\Gamma} q^*(\mathbf{x},\mathbf{y})\, u(\mathbf{y})\, d\Gamma = \int_{\Gamma} u^*(\mathbf{x},\mathbf{y})\, q(\mathbf{y})\, d\Gamma + \int_{\Omega} u^*(\mathbf{x},\mathbf{y})\, b(\mathbf{y})\, d\Omega \tag{8}$$

Here, u* is the fundamental solution which is the solution to the adjoint of the governing partial differential equation which satisfies the homogeneous boundary conditions in an infinite domain [26].
After discretization using BEM, there will be $N_{BN}+N_{INT}$ boundary integral equations, one for each boundary node N_{BN} plus one for every internal temperature measurement N_{INT}. The resulting discretized version of the BEM can be represented in matrix form as

$$[\mathbf{H}]\{\mathbf{U}\} = [\mathbf{G}]\{\mathbf{Q}\} + [\mathbf{R}]\{\mathbf{B}\} \tag{9}$$

where [**H**], [**G**] and [**R**] are the geometric coefficient matrices. For example, if at two vertices (1 and 3) of a quadrilateral surface panel both $u = \bar{u}$ and $q = \bar{q}$ are known, while at the remaining two vertices (2 and 4) neither quantity is known, the BIE equation set begins as

$$\begin{bmatrix} h_{11} & h_{12} & h_{13} & h_{14} \\ h_{21} & h_{22} & h_{23} & h_{24} \\ h_{31} & h_{32} & h_{33} & h_{34} \\ h_{41} & h_{42} & h_{43} & h_{44} \end{bmatrix} \begin{Bmatrix} \bar{u}_1 \\ u_2 \\ \bar{u}_3 \\ u_4 \end{Bmatrix} = \begin{bmatrix} g_{11} & g_{12} & g_{13} & g_{14} \\ g_{21} & g_{22} & g_{23} & g_{24} \\ g_{31} & g_{32} & g_{33} & g_{34} \\ g_{41} & g_{42} & g_{43} & g_{44} \end{bmatrix} \begin{Bmatrix} \bar{q}_1 \\ q_2 \\ \bar{q}_3 \\ q_4 \end{Bmatrix} + \begin{bmatrix} r_{11} & r_{12} & r_{13} & r_{14} \\ r_{21} & r_{22} & r_{23} & r_{24} \\ r_{31} & r_{32} & r_{33} & r_{34} \\ r_{41} & r_{42} & r_{43} & r_{44} \end{bmatrix} \begin{Bmatrix} \bar{b}_1 \\ \bar{b}_2 \\ \bar{b}_3 \\ \bar{b}_4 \end{Bmatrix} \tag{10}$$

For a well-posed boundary condition problem, every point on the boundary is given either one Dirichlet, one Neumann or one Robin boundary condition assuming that internal heat source distribution is known. Additional equations may be added to this equation set if temperature measurements are known at certain locations within the domain. The known nodal variables are then multiplied by their respective coefficient matrix terms and transferred to the right hand side [3,4,5]. Similarly, all unknown nodal variables are multiplied by their respective coefficient matrix terms and transferred to the left hand side.

$$\begin{bmatrix} h_{12} & -g_{12} & h_{14} & -g_{14} \\ h_{22} & -g_{22} & h_{24} & -g_{24} \\ h_{32} & -g_{32} & h_{34} & -g_{34} \\ h_{42} & -g_{42} & h_{44} & -g_{44} \end{bmatrix} \begin{Bmatrix} u_2 \\ q_2 \\ u_4 \\ q_4 \end{Bmatrix} = \begin{bmatrix} -h_{11} & g_{11} & -h_{13} & g_{13} \\ -h_{21} & g_{21} & -h_{23} & g_{23} \\ -h_{31} & g_{31} & -h_{33} & g_{33} \\ -h_{41} & g_{41} & -h_{43} & g_{43} \end{bmatrix} \begin{Bmatrix} \bar{u}_1 \\ \bar{q}_1 \\ \bar{u}_3 \\ \bar{q}_3 \end{Bmatrix} + \begin{bmatrix} p_{11} & p_{12} & p_{13} & p_{14} \\ p_{21} & p_{22} & p_{23} & p_{24} \\ p_{31} & p_{32} & p_{33} & p_{34} \\ p_{41} & p_{42} & p_{43} & p_{44} \end{bmatrix} \begin{Bmatrix} \bar{b}_1 \\ \bar{b}_2 \\ \bar{b}_3 \\ \bar{b}_4 \end{Bmatrix} \tag{11}$$

The result is a standard linear matrix form of the general type [**A**]{**X**}={**F**}. This well-posed system of linear algebraic equations can be solved for the vector of unknown values {**X**} at the boundary points by any standard matrix solver such as Gaussian elimination or LU factorization. Once the boundary temperatures and heat fluxes are determined, the surface variation of h_{conv} is readily available from Eq. (2) [6].

DETERMINATION OF STEADY BOUNDARY CONDITIONS IN ELASTICITY USING BEM

Well-posed (analysis or forward) problems in steady-state elasticity require knowledge of either

displacement vectors, **u**, or surface traction vectors, **p**, everywhere on the surface of the solid body. When performing an inverse evaluation of the steady-state elasticity problem using the BEM, both **u** and **p** are unknown on a part of the solid's surface. Elsewhere on the solid's surface, either **u** or **p** should be applied, while both **u** and **p** must be specified on at least some parts of the surface. The surface section where both **u** and **p** are specified simultaneously is called the over-specified boundary

The state of stress at a point is defined using a symmetrical stress tensor, σ. The stress components must satisfy the following equilibrium equations throughout the interior of the solid body.

$$\frac{\partial \sigma_{kj}}{\partial x_j} + b_k = 0 \tag{12}$$

where j =1,2 and k = 1,2 and b_k are the net body forces per unit volume. These forces could be caused by thermal stresses. The surface force tractions on the object are denoted by the vector, p_k , and the prescribed boundary values of these tractions on the surface Γ_p are denoted by P_k .. Let Γ_u be the portion of the boundary where the displacement boundary conditions, U_k , are prescribed while where u_k is the vector displacement field. The principle of virtual displacements for linear elastic problems can be written as [11],

$$\int_\Omega \left(\frac{\partial \sigma_{kj}}{\partial x_j} + b_k \right) u_k^* \, d\Omega = \int_{\Gamma_p} (p_k - P_k) u_k^* \, d\Gamma + \int_{\Gamma_u} (U_k - u_k) p_k^* \, d\Gamma \tag{13}$$

where p_k * are the surface tractions corresponding to the virtual displacements, u_k *. The boundary Γ is discretized into N_{sp} surface panels connected between N nodes. The functions **u** and **p** are quadratically distributed over each panel with adjacent panels sharing nodes such that there will be twice as many boundary nodes as there are surface panels. The displacements and tractions are defined in terms of three nodal values and three quadratic interpolation functions. The whole set of boundary integral equations can be written in a matrix form as

$$[\mathbf{H}] \{\mathbf{U}\} = [\mathbf{G}] \{\mathbf{P}\} \tag{14}$$

where the vectors {**U**} and {**P**} contain the nodal values of the displacement and traction vectors. Each entry in the [**H**] and [**G**] matrices is developed by properly summing the contributions from each numerically integrated surface integral. The set of boundary integral equations will contain a total of 2N equations and 6N nodal values of displacements and surface tractions.

For a well-posed boundary value problem, at least one of the functions, **u** or **p**, will be known at each boundary node (either Dirichlet or von Neumann boundary condition) so that the equation set will be composed of 2N equations and 2N unknowns. For an ill-posed boundary value problem, both **u** and **p** should be enforced simultaneously at certain boundary nodes, while either **u** or **p** should be enforced at the other boundary nodes, and nothing enforced at the remaining boundary nodes since no boundary values are known there. If at two boundary nodes (1 and 3) of a quadrilateral boundary element both **u** = **U** and **p** = **P** are known, but at the other two nodes (2 and 4) neither **u** nor **p** is known, all the known quantities can be transferred to the RHS so that the BEM equation set after this rearrangement appears as [2]

$$\begin{bmatrix} \mathbf{h}_{12} & -\mathbf{g}_{12} & \mathbf{h}_{14} & -\mathbf{g}_{14} \\ \mathbf{h}_{22} & -\mathbf{g}_{22} & \mathbf{h}_{24} & -\mathbf{g}_{24} \\ \mathbf{h}_{32} & -\mathbf{g}_{32} & \mathbf{h}_{34} & -\mathbf{g}_{34} \\ \mathbf{h}_{42} & -\mathbf{g}_{42} & \mathbf{h}_{44} & -\mathbf{g}_{44} \end{bmatrix} \begin{Bmatrix} \mathbf{u}_2 \\ \mathbf{p}_2 \\ \mathbf{u}_4 \\ \mathbf{p}_4 \end{Bmatrix} = \begin{bmatrix} -\mathbf{h}_{11} & \mathbf{g}_{11} & -\mathbf{h}_{13} & \mathbf{g}_{13} \\ -\mathbf{h}_{21} & \mathbf{g}_{21} & -\mathbf{h}_{23} & \mathbf{g}_{23} \\ -\mathbf{h}_{31} & \mathbf{g}_{31} & -\mathbf{h}_{33} & \mathbf{g}_{33} \\ -\mathbf{h}_{41} & \mathbf{g}_{41} & -\mathbf{h}_{43} & \mathbf{g}_{43} \end{bmatrix} \begin{Bmatrix} \mathbf{U}_1 \\ \mathbf{P}_1 \\ \mathbf{P}_3 \\ \mathbf{P}_3 \end{Bmatrix} = \begin{Bmatrix} \mathbf{f}_1 \\ \mathbf{f}_2 \\ \mathbf{f}_3 \\ \mathbf{f}_4 \end{Bmatrix} \tag{15}$$

where each of the entries in the [**H**] and [**G**] matrices is a 2x2 submatrix in the case of a two-dimensional

domain. The right-hand side vector {**F**} is known and the left-hand side remains in the form [**A**]{**X**}. Additional equations may be added to the equation set if deformation measurements, **u**, are known at locations within the solid in order to enhance the accuracy of the inverse steady boundary condition algorithm. A proper physical solution will be obtained if the number of equations equals or exceeds the number of unknowns. If the number of equations is less than the number of unknowns, the Singular Value Decomposition (SVD) method will find one solution [14], although it does not necessarily have to be the proper solution from the physical point of view.

REMARKS ON SVD ALGORITHM AND TIKHONOV'S REGULARIZATION

Thus, if the boundary conditions (T, q, or h_{conv}) are unknown on parts of the boundary or if internal temperature measurements are included in the analysis, the problem becomes ill-posed. However, a solution may still be obtained by multiplying the known quantities in the vectors {**U**} and {**Q**} by their respective coefficient matrix columns and collecting them into the vector of knowns, {**F**}. All the unknowns then form a single vector, {**X**}, multiplied by a highly ill-conditioned coefficient matrix, [**A**], which is, in general, not square. The truncated SVD method [14,15] has been often used to solve this ill-conditioned system of algebraic equations. In order to determine which singular values in [**A**] are to be truncated, we must choose a user-specified singularity threshold parameter, τ_{SVD}. Any singular value, whose ratio with the largest singular value is less than this singularity threshold, is zeroed out. The objective is that those algebraic terms that are dominated by noise and round-off error are eliminated from the matrix.

Tikhonov's regularization [13] is another type of single-parameter minimization where the solution vector {**X**} minimizes the weighted sum of the norm of the error vector plus a penalty term. Tikhonov's regularization is actually a generalization of least-squares truncation. Instead of eliminating terms associated with small singular values, they are weighted by a factor $(1 + \tau_{TIH} / \omega^2)$ where ω is any of the singular values of the matrix [**A**]. Of crucial importance in this approach is the magnitude of the Tikhonov's regularization parameter, τ_{TIH}. A low value makes the residual term [**A**]{**X**}-{**F**} smaller thus approaching the least squares solution. However, since the small singular values are associated with noise, the solution for an ill-conditioned matrix often oscillates erratically. Larger Tikhonov's regularization parameters act as a filter to gradually reduce the effect of the singular values because ω_j/ω_{max} are less than the regularization parameter, τ_{TIH}. Large values of this parameter create results that are very smooth, but also increasingly wrong. However, there is no general formulation for determining an optimal choice of the regularization parameter that provides a balance between the smoothness and the accuracy of the solution [4].

We have performed detailed testing of both SVD and Tikhonov's regularization in a number of test cases involving heat conduction inverse boundary condition problems [4-9]. Contrary to the widely accepted beliefs, we observed that Tikhonov's regularization produces smooth results, but often generates unacceptable levels of global error [4].

FINITE ELEMENT METHOD FORMULATION

Our objective is to demonstrate that the same general concept used with BEM formulation is also applicable when using the FEM formulation in prediction of thermal and elasticity boundary conditions.

FEM formulation with Galerkin's method [12]after assembling all element equations results in two linear algebraic systems that could be expressed (in case of no heat sources) as

$$[K_c]\{u\} = \{q\} \quad \text{and} \quad [K]\{\delta\} = \{f\} \tag{16}$$

Here, $[K_c]$is the stiffness matrix for the thermal problem and $[K]$is the stiffness matrix for the elasticity problem. Similarly, $\{u\}$is the vector of unknown Kirchoff's temperature functions and $\{\delta\}$ is the vector of the unknown deformations (displacements). Both of these systems are typically large and sparse, but they are also symmetric and positive definite. For example, thermal problem formulation results in

$$\begin{bmatrix} K_{C11} & K_{C12} & K_{C13} & K_{C14} \\ K_{C21} & K_{C22} & K_{C23} & K_{C24} \\ K_{C31} & K_{C32} & K_{C33} & K_{C34} \\ K_{C41} & K_{C42} & K_{C43} & K_{C44} \end{bmatrix} \begin{Bmatrix} u_1 \\ u_2 \\ u_3 \\ u_4 \end{Bmatrix} = \begin{Bmatrix} q_1 \\ q_2 \\ q_3 \\ q_4 \end{Bmatrix} \tag{17}$$

In the case of an ill-posed problem, thermal and elasticity boundary conditions will not be known on some parts of the boundary. For example, in three-dimensional heat conduction while using a tetrahedral (three-dimensional) finite element, one could specify both the temperature, u_s, and the heat flux, q_s, at node 1, flux only at nodes 2 and 3, and assume the boundary conditions at node 4 as unknown. The original system of linear algebraic equations is modified by adding a row and a column corresponding to the additional equation for the over-specified flux at node 1 and the additional unknown due to the unknown boundary flux at node 4 [7-10].

$$\begin{bmatrix} 1 & 0 & 0 & 0 & 0 \\ K_{C21} & K_{C22} & K_{C23} & K_{C24} & 0 \\ K_{C31} & K_{C32} & K_{C33} & K_{C34} & 0 \\ K_{C41} & K_{C42} & K_{C43} & K_{C44} & -1 \\ K_{C11} & K_{C12} & K_{C13} & K_{C14} & 0 \end{bmatrix} \begin{Bmatrix} u_1 \\ u_2 \\ u_3 \\ u_4 \\ q_4 \end{Bmatrix} = \begin{Bmatrix} u_{1s} \\ q_2 \\ q_3 \\ 0 \\ q_{1s} \end{Bmatrix} \tag{18}$$

A similar procedure is also applied to the elasticity system of equations [7-10] where thermal stresses are accounted for in the vector $\{F\}$. These linear systems will remain sparse (since FEM creates sparse matrix problems), but will be non-symmetric and possibly rectangular depending on the ratio of the actual number of known to unknown boundary conditions. These systems can be solved by a variety of methods, but sparse solvers are usually required for minimizing memory requirements. Resulting systems are usually ill-conditioned due to the nature of the inverse problem. The degree of ill-conditioning depends on the geometry, ratio of the number of known to unknown boundary values, level of noise in the boundary data provided, etc. Since the entire FEM approach is iterative, the ill-conditioning would result in an uncontrolled growth of errors. Therefore, it is of a crucial importance to employ an appropriate algorithm that will smooth (regularize) these errors.

REGULARIZATION FORMULATIONS

A regularization method was applied to the solution of the systems of equations in an attempt to increase the method's tolerance to possible measurement errors in the over-specified boundary conditions.
For example, in case of the thermal problem the general form of the regularized system is given as

$$\begin{bmatrix} K_C \\ \lambda D \end{bmatrix} \{u\} = \begin{Bmatrix} q \\ 0 \end{Bmatrix} \tag{19}$$

The form of the damping matrix $[D]$ determines what penalty is used. The damping parameter, Λ, weights the penalty for each equation. Notice that $[D] = [I]$ corresponds to traditional Tikhonov's regularization. If it is explicitly stated that $\Lambda = 0$ for all equations involving only interior points while $[D] = [I]$ is used only for equations involving the unknown boundary values, then the results will be smooth and the error explicitly introduced by the regularization will be small [7-9].
An even more advanced regularization formulation minimizes the Laplacian of the unknown boundary values [8,9]. This provides a smoothing of the temperatures without driving them to zero. Thus, the damping matrix can be interpreted as an assembly of boundary elements on the boundary where the temperatures are unknown. In case of an inverse thermal problem the method of weighted residuals can be used to form a discrete Laplacian operator for the boundary elements.

$$\left\|\nabla^2 u\right\|_2^2 \rightarrow min \tag{20}$$

In the case of elasticity, the following version of regularization of the boundary values has been used [9]

$$\left\|\nabla^2 \left(\hat{n} \cdot \{\delta\}\right)\right\|_2^2 \rightarrow min \tag{21}$$

If both of these equations are discretized using a method of weighted residuals, the appropriate damping matrix can be determined for the combined inverse thermo-elasticity problems from the following formula applied at boundary points only [22]

$$\left\|[D]u\right\|_2^2 = \left\|[K_C]u\right\|_2^2 \tag{22}$$

For each boundary element on unknown boundary we transform Laplace's equation to natural surface-following coordinates, discretize Laplace's equation using Galerkin's method, compute local damping matrix [*D*], and assemble [*D*] into a global damping matrix. Standard sparse solvers can be used to solve these normalized systems, but such systems are usually highly ill-conditioned. Direct or iterative sparse solvers for least-squares problems can also be used. Examples are sparse QR factorization and LSQR iterative method. Iterative methods are difficult to use in practice since they require good preconditioners for fast convergence. Use of static condensation method for decreasing the sparseness of the matrix and then use of a dense rectangular solver such as SVD to solve for the unknowns on the boundary is also an option [15].

NUMERICAL EXAMPLES

The accuracy and efficiency of the FEM inverse formulation was tested on a simple three-dimensional electronic package [10] known as ball grid assembly (BGA) (Fig. 1). A forward problem (direct or well-posed problem) was solved to generate the over-specified boundary conditions for the inverse problem. In this example, the objective was to inversely determine the junction temperature on the bottom surface of the die by using only measurements on the outside of the electronic package. Only one quarter of the package was modeled due to symmetry in shape and boundary conditions where 33 solder balls are used in the ¼ model. The grid is composed of 27,417 nodes and 20,728 elements. Hexahedral (brick) elements with tri-linear interpolation functions were used instead of tetrahedra to improve accuracy in the thin material layers (Fig. 2).

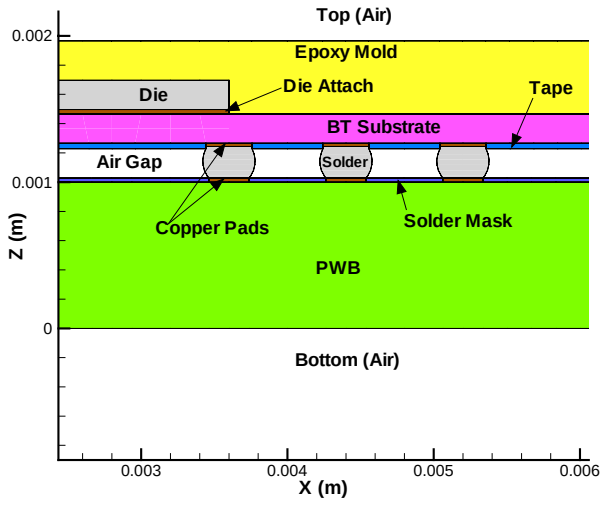

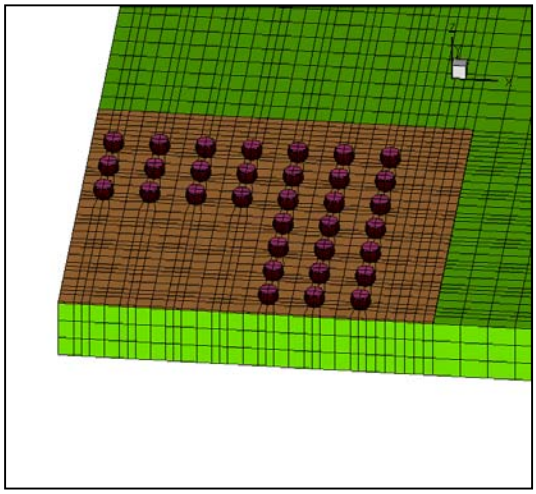

Fig. 1 A cross-section of the BGA electronic package. *Fig. 2 Computational grid for the BGA detail.*

Sparse QR factorization was used to solve the linear system in all cases. The model was made up of nine material regions (Table 1) and maintains the characteristic size, shape, and materials of a typical BGA (Table 2). Convection (Robin) type boundary conditions were used on all surfaces. The forward (well-posed analysis) problem was solved using all model regions. Die dissipates 0.75 Watts of power, assumed to be uniformly distributed, so that a value of 0.1875 was used for the ¼ model.

Table 1. Thermal conductivities of the nine materials used.

Region	Material	$k_x, k_y, k_z\ (W/m^oC)$
1	FR4 printed wire board (FWB)	1.0, 1.0, 0.3
2	copper pads	393.0, 393.0, 393.0
3	solder mask	0.2, 0.2, 0.2
4	polyimide tape	0.3, 0.3, 0.3
5	solder balls	250.0, 250.0, 250.0
6	bismaleimide triazene (BT) substrate	1.0, 1.0, 0.3
7	die attach	0.25, 0.25, 0.25
8	silicon die	87.0, 87.0, 87.0
9	epoxy mold compound (EMC)	0.71, 0.71, 0.71

Table 2. Thermal boundary conditions.

Boundary	$\Theta_{amb}\ (^oC)$	$h\ (W/m^{2o}C)$
Symmetry	0.0	0.0
All sides of PWB	25.0	19.71
Top and sides of package	25.0	43.18
Bottom of package	25.0	4.31
Sides of solder balls	0.0	0.0

The inverse problem was created by over-specifying the boundary conditions on the top and sides of the epoxy package. No boundary conditions were applied to the bottom of the substrate. Thus, the objective was to determine die junction temperature using measurements on the outside of the epoxy mold. The substrate bottom is not accessible, so conditions there are unknown.

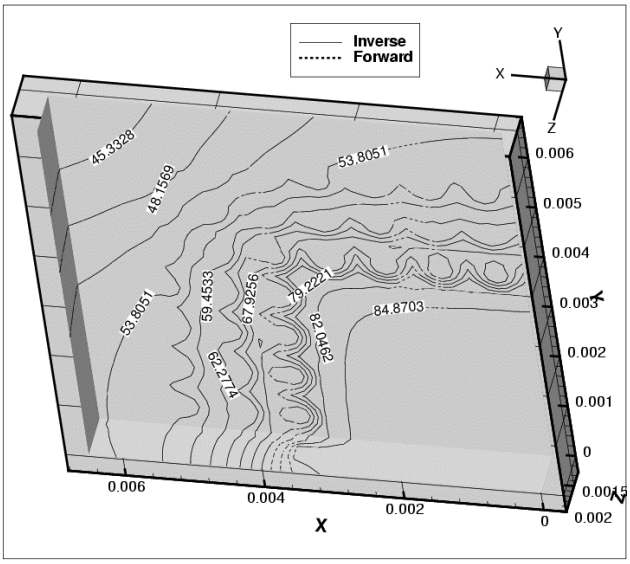

Fig. 3. Bottom of substrate: isotherms from inverse and forward solutions with no measurement errors and $\Lambda = 10^{-30}$.

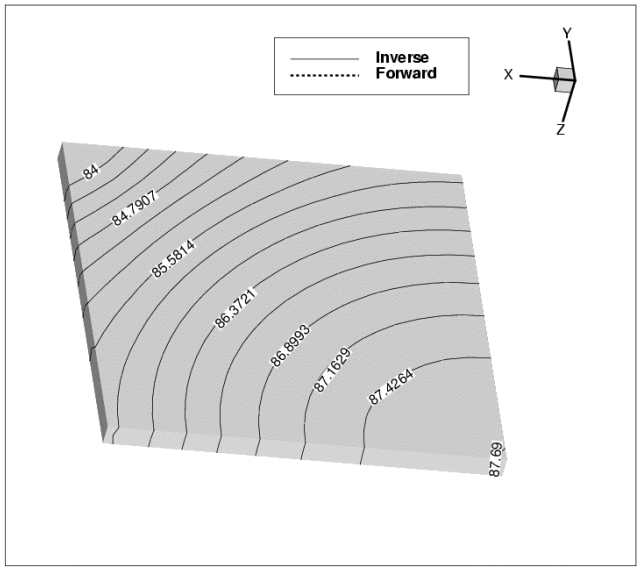

Fig. 4. Bottom of dye: isotherms from inverse and forward solutions with no measurement errors and $\Lambda = 10^{-30}$.

Inverse determination of the junction temperature on the surface of the silicon die was accomplished economically by modeling only regions 6-9 (9800 nodes). Results of inverse analysis without a provision for measurement errors are in Fig. 3 and Fig. 4 demonstrating very high accuracy of this inverse algorithm. The measurement errors were then simulated by taking temperatures and fluxes on the epoxy package from the forward problem and applying a random error with $\sigma = 0.01$. For $\sigma = 0.01$, the average error in over-specified temperature was 1.27% (Fig. 5) and average flux error was 1.24%. With a considerably different value of Λ (Fig. 6) the inverse results for this realistic problem were very good (Figs. 7 and 8).

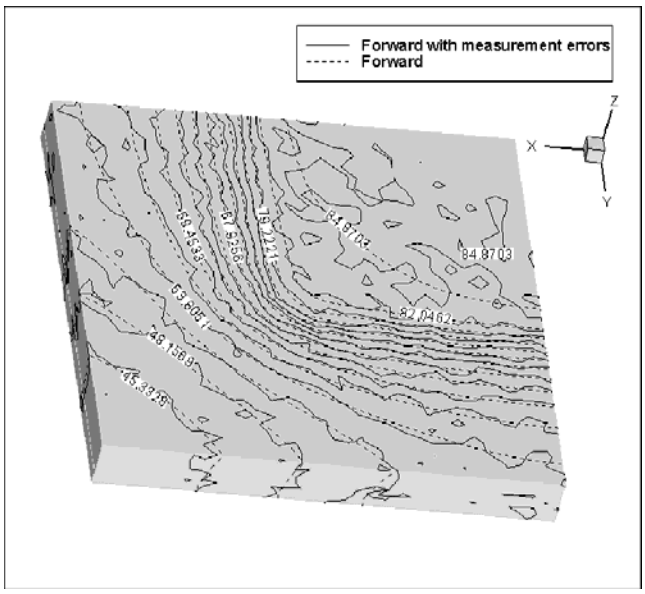

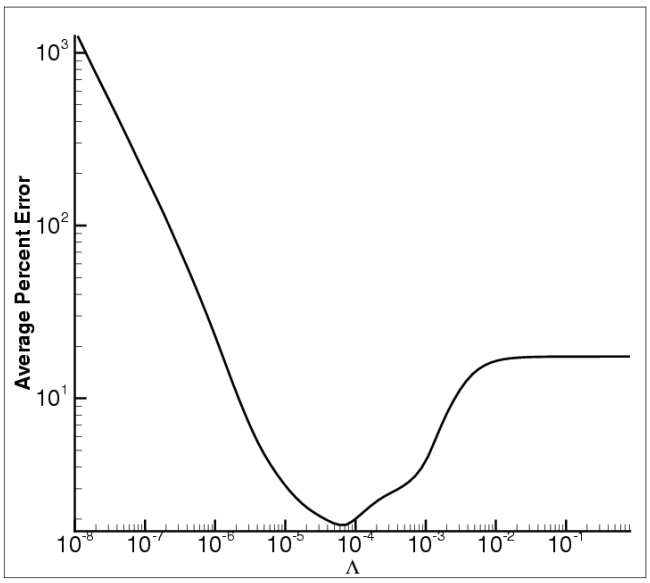

Fig. 5. Top of epoxy package: temperature distribution used without and with simulated mean random errors of 1.27% in overspecified temperature and 1.24% in overspecified heat flux .

Fig. 6. Temperature error on substrate bottom as a function of damping parameter. The temperature error on the substrate bottom was less than 3.0% for $10^{-5}<\Lambda<10^{-3}$.

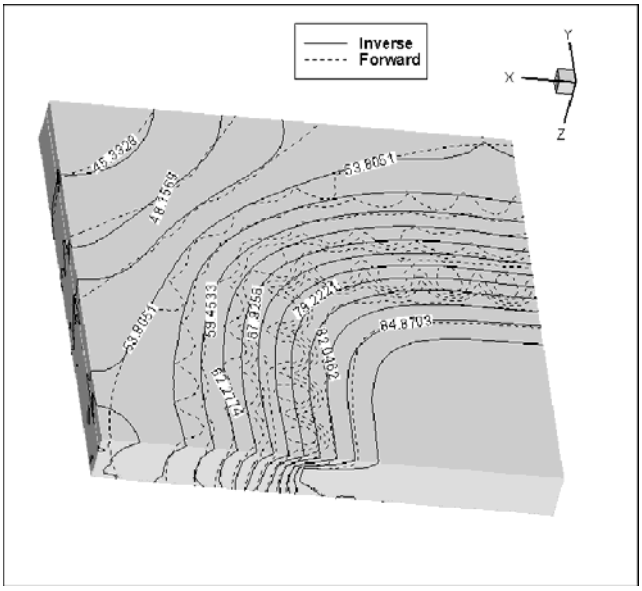

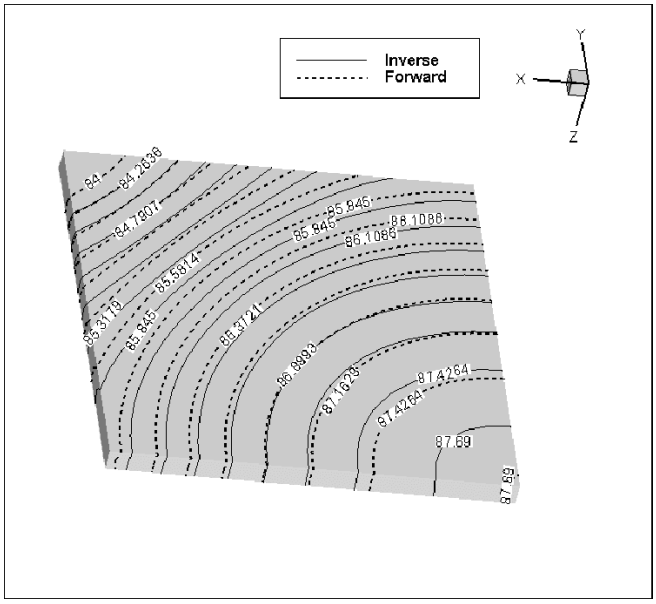

Fig. 7. Bottom of substrate: isotherms from inverse and forward solutions when measurement errors were used on boundaries and with $\Lambda = 10^{-4}$.

Fig. 8. Bottom of dye: isotherms from inverse and forward solutions when measurement errors were used on boundaries and with $\Lambda = 10^{-4}$.

SUMMARY

The BEM and FEM formulations for inverse determination of unknown steady boundary conditions in multi-dimensional heat conduction and elasticity were summarized. The formulations are applicable to arbitrarily shaped multiply connected objects made of different materials. It was demonstrated that these inverse methods can predict boundary values with high accuracy.

ACKNOWLEDGEMENTS

The first author is grateful for the partial support provided for this research from the grant NSF DMS-0073698 administered through the Computational Mathematics program. The second author is grateful for the support for this research from the Graduate School of Frontier Sciences at the University of Tokyo.

REFERENCES

[1] G. S. Dulikravich, *Inverse design and active control concepts in strong unsteady heat conduction*, Applied Mechanics Reviews, 41, (6) (1988) 270-277.

[2] T. J. Martin, J. Halderman, J., G. S. Dulikravich, *An inverse method for finding unknown surface tractions and deformations in elastostatics*, Symposium on Inverse Problems in Mechanics, ASME Winter Annual Meeting, Chicago, IL, November 6-11, 1994; S. Saigal, L. G. Olson, eds., ASME AMD-Vol. 186, pp. 57-66; also in *Computers and Structures*, 56, (5) (1995) 825-836.

[3] G. S. Dulikravich, T. J. Martin, *Finding temperatures and heat fluxes on inaccessible surfaces in 3-d coated rocket nozzles, Proceedings of 1995 JANNAF Propulsion and Subcommittee Joint Meeting*, Tampa, FL, Dec. 4-8 (1995)

[4] T. J. Martin, T. J., G. S. Dulikravich, *Inverse determination of boundary conditions in steady heat conduction with heat generation*, ASME Journal of Heat Transfer, 118, (3) (1996) 546-554.

[5] G. S. Dulikravich, T. J. Martin, *Inverse shape and boundary condition problems and optimization in heat conduction*, Chapter no. 10 in *Advances in Numerical Heat Transfer - Volume I* , W. J. Minkowycz E. M. Sparrow, eds., Taylor and Francis, (1996) 381-426.

[6] T. J. Martin, G. S. Dulikravich, *Inverse determination of steady heat convection coefficient distributions*, ASME J. of Heat Transfer, 120, (1998) 328-334.

[7] B. H. Dennis, G. S. Dulikravich, *Simultaneous determination of temperatures, heat fluxes, deformations, and tractions on inaccessible boundaries*, ASME J. of Heat Transfer, 121, (1999) 537-545.

[8] B. H. Dennis, G. S. Dulikravich, *Simultaneous determination of temperatures, heat fluxes, deformations, and tractions on inaccessible boundaries*, Symposium on Inverse Problems in Mechanics, ASME IMECE'98, L. G. Olson, S. Saigal, eds., Anaheim, CA, Nov. 15-20, 1998, ASME AMD-Vol. 228, pp. 1-10: also in ASME Journal of Heat Transfer, 121, (1999) 537-545.

[9] B. H. Dennis, G. S. Dulikravich, *A finite element formulation for the determination of unknown boundary conditions for three-dimensional steady thermoelastic problems*, ASME J. of Heat Transfer, 126, (2004) 110-118.

[10] B. H. Dennis, Z. X. Han, G. S. Dulikravich, *Determination of temperatures and heat fluxes on surfaces and interfaces of multi-domain three-dimensional electronic components*, ASME paper IMECE2003-42273, Symposium on Cooling of Microelectronics, MEMS, Photonics, and Nano Devices, ASME IMECE 2003, Washington, DC, Nov. 16-21 (2003).

[11] C. A. Brebbia, J. Dominguez, *Boundary Elements, An Introductory Course,* McGraw-Hill Book Company, New York (1989).

[12] T. J. R. Hughes, *The Finite Element Method: Linear Static and Dynamic Finite Element Analysis*, Dover Publications, Inc., New York (2000).

[13] A. N. Tikhonov, *Solutions of Ill-Posed Problems*, Halsted Press, Washington: Winston: New York (1997).

[14] W. H. Press, S. A. Teukolsky, W. T. Vetterling, B. P. Flannery, *Numerical Recipes in FORTRAN: The Art of Scientific Computing*, 2nd Ed., Cambridge Univ. Press (1992).

[15] L. G. Olson, R. D. Throne, *The steady inverse heat conduction problem: A comparison for methods for methods of inverse parameter selection*, ASME paper NHTC2000-12022, 34th ASME National Heat Transfer conference, Pittsburgh, PA (2000).